

Mechanism of C₄ Photosynthesis

THE SIZE AND COMPOSITION OF THE INORGANIC CARBON POOL IN BUNDLE SHEATH CELLS

Received for publication May 19, 1987 and in revised form July 16, 1987

ROBERT T. FURBANK AND MARSHALL D. HATCH*

Division of Plant Industry, CSIRO, G.P.O. Box 1600, Canberra, A.C.T. 2601, Australia

ABSTRACT

We sought to characterize the inorganic carbon pool (CO₂ plus HCO₃⁻) formed in the leaves of C₄ plants when C₄ acids derived from CO₂ assimilation in mesophyll cells are decarboxylated in bundle sheath cells. The size and kinetics of labeling of this pool was determined in six species representative of the three metabolic subgroups of C₄ plants. The kinetics of labeling of the inorganic carbon pool of leaves photosynthesizing under steady state conditions in ¹⁴CO₂ closely paralleled those for the C-4 carboxyl of C₄ acids for all species tested. The inorganic carbon pool size, determined from its ¹⁴C content at radioactivity saturation, ranged between 15 and 97 nanomoles per milligram of leaf chlorophyll, giving estimated concentrations in bundle sheath cells of between 160 and 990 micromolar. The size of the pool decreased, together with photosynthesis, as light was reduced from 900 to 95 microeinsteins per square meter per second or as external CO₂ was reduced from 400 to 98 microliters per liter. A model is developed which suggests that the inorganic carbon pool existing in the bundle sheath cells of C₄ plants during steady state photosynthesis will comprise largely of CO₂; that is, CO₂ will only partially equilibrate with bicarbonate. This predominance of CO₂ is believed to be vital for the proper functioning of the C₄ pathway.

from the C-4 carboxyl of malate or aspartate. Its size indicated a bundle sheath CO₂ plus HCO₃⁻ concentration of up to 1 mM.

The aim of the present study was to examine the characteristics of the inorganic carbon pool developed in a wider variety of C₄ plants. Species representing the three subtypes of C₄ plants (14) were examined and the effect of varying light and external CO₂ concentration of the size leaf CO₂ pool was also determined. A model is developed which predicts the likely ratios of CO₂ to HCO₃⁻ existing in bundle sheath cells during steady state photosynthesis.

MATERIALS AND METHODS

Leaf Material. Plants were grown in soil in a naturally illuminated greenhouse maintained between 20 and 30°C. The species examined were: *Sorghum sudanense*, *Echinochloa crus-galli*, *Eleusine indica*, *Panicum miliaceum*, *Urochloa panicoides*, *Panicum maximum*, *Phalaris tuberosa*. High specific activity Ba ¹⁴CO₃ (55 mCi mmol⁻¹) was obtained from Amersham (Australia). Biochemicals and enzymes were obtained from Sigma Chemical Co. or Boehringer-Mannheim (Australia).

Leaf ¹⁴CO₂ Labeling Experiments. Fully expanded leaves from 4- to 6-week old plants were removed and then recut under water to give segments from the midportion about 15 cm long. Using a similar procedure to that previously described (10, 15) six leaves were placed in a 3 L perspex chamber (with their basal end dipping in a trough of water) which was flushed with humidified air (about 350 μl CO₂ L⁻¹) at a flow rate of about 10 L min⁻¹. The gas phase was stirred with two high speed fans fixed into the end walls of the chamber (air temperature about 25°C). Leaves were illuminated (900 μE m⁻² s⁻¹ PAR unless otherwise specified) with a 400 W Phillips HLG lamp for about 30 min to allow a steady rate of photosynthesis to develop. Experiments were then commenced by sealing the chamber and injecting about 0.75 mCi of ¹⁴CO₂ gas which elevated the CO₂ concentration from 350 μl L⁻¹ to about 400 μl L⁻¹. At intervals, individual leaves were withdrawn through a rubber gasket and immediately killed in the light by plunging into 30 ml of 85% ethanol containing 0.03% (w/v) 2,4 dinitrophenylhydrazine and 100 mM trifluoroacetic acid in a large test tube kept at -80°C in a mixture of ethanol and solid carbon dioxide. As previously described (10) the tubes were immediately tightly sealed with special stoppers (sealed channels for air inlet and outlet), stored for at least 24 h at -20°C to allow complete penetration of the reagent mixture, and then the ¹⁴CO₂ gas present was trapped in 0.3 M hyamine hydroxide in ethanol. Procedures used to extract leaves and to separate the soluble, insoluble (starch), and hydrazone fractions, and to measure the phaeophytin content of the leaf samples, were as previously described (10). The radioactivity of the various fractions was determined by liquid scintillation counting.

Light was varied by altering the distance of the leaf chamber from the light source specified above. Where the CO₂ concentration in the chamber was varied the mixtures containing lower

There is now a great deal of indirect evidence to support the original proposal (4, 9) that the primary function of the unique reactions of the C₄ pathway is to concentrate CO₂ in bundle sheath cells. A high CO₂ concentration in bundle sheath cell is believed to be one of the critical factors accounting for the various physiological features typical of C₄ plants such as their high light saturated photosynthetic rates, high quantum yield, the absence of effects of oxygen on photosynthesis, and their apparently negligible photorespiration (6, 14). These features are assumed to result from the combination of high PEP¹ carboxylase activity in mesophyll cells, giving high rates of initial CO₂ assimilation into C₄ acids, and of RuBP carboxylase operating in the bundle sheath cells in an environment where the high CO₂ to O₂ ratio gives maximum rates of assimilation with negligible oxygenase activity. Although this CO₂ concentrating role is central to explaining the function of C₄ photosynthesis there is only one report providing direct experimental evidence for the existence of a large inorganic carbon pool in C₄ leaves during photosynthesis (10). In that study the radioactive pool of CO₂ plus HCO₃⁻ in leaves of *Zea mays* and *Amaranthus edulis* was measured during assimilation of ¹⁴CO₂ under steady state conditions for photosynthesis. The results supported the concept of a large CO₂ pool with the labeling kinetics consistent with it being derived

¹ Abbreviations: PEP, phosphoenolpyruvate; RuBP, ribulose 1,5-bisphosphate; 3-PGA, 3-phosphoglycerate.

CO₂ concentrations were generated by mixing normal air with CO₂-free air through flow meters. The CO₂ concentration in the mixtures was monitored with an infrared CO₂ analyzer. For these and other studies, the ¹⁴C content of the chamber gas phase was determined by removing a 2 ml sample with a syringe and trapping the ¹⁴CO₂ by injecting the sample into a flask containing 10 ml of 0.3 M hyamine hydroxide in ethanol.

Determination of Radioactivity in Photosynthetic Intermediates and Products. After extracting pheophytin and hydrazones, the residual aqueous extract of leaves was evaporated to dryness and then dissolved in about 1.5 ml of water and stored at -20°C. Samples of this extract were chromatographed on Whatman 3MM paper using 2-butanol:formic acid:water, 6:1:2 (by volume) as the developing solvent (adapted from Schürmann [25]). The proportions of total radioactivity in malate, alanine, glycerate 3-phosphoglycerate, sucrose, and combined sugar phosphates were determined from the peaks traced with a radiochromatogram scanner. Radioactive malate eluted from these chromatograms with water was used to determine the proportion of total ¹⁴C in the C-4 carboxyl group. The amino acid fraction of the soluble extract was isolated by chromatography on a column of Bio-Rad AG-50W-X8 as previously described (11). Proportions of the total ¹⁴C in individual amino acids was determined by chromatographing samples of this fraction on Whatman 3MM paper developed first for 6 h at 25°C with acetone:water:diethylamine, 80:15:5 (v/v) and, after drying, with pyridine:acetic acid:water, 50:35:15 (v/v) for 14 h at 25°C (18). This procedure separated radioactive aspartate, glutamate, glycine, serine, and alanine. The radioactive aspartate eluted from these chromatograms with water was used to determine the proportion of total label in the C-4 carboxyl (see below).

Radioactive malate was degraded with NADP malic enzyme (11), and aspartate with aspartate decarboxylase (10) to determine the proportion of total radioactivity in the C-4 carboxyl group.

Calculation of Photosynthetic Rates, Metabolite Pool Sizes, and Cellular Concentrations. Photosynthetic rates were determined from the amount of ¹⁴CO₂ of known specific activity assimilated by leaves. The size of the pools of inorganic carbon and C₄ acids was determined on the assumption that when the labeling of a particular carbon reached a plateau level (the C-4 carboxyl in the case of C₄ acids) then the specific activity would be equivalent to that of the supplied ¹⁴CO₂.

Values used for estimating the inorganic carbon pool concentrations in Table I were derived as follows. An average value of 19% was used for the proportion of leaf volume occupied by bundle sheath cells based on the proportion of leaf cross-sectional area occupied by bundle sheath cells in light micrographs (average for six grass species, range 15–24%). The value of 50% for the cytosolic component (including chloroplasts and mitochondria) of cell volume was based on the average area occupied by cytosol in electron micrographs of bundle sheath cells determined for five grass species (S Craig, unpublished data, range 40–63%). The value for stromal volume of 25 μl mg⁻¹ Chl was an average of published values. The Chl content of 2 mg g⁻¹ fresh weight of leaf was the average determined for three grass species (range 1.85–2.05 mg g⁻¹ fresh weight).

RESULTS

Kinetics of ¹⁴CO₂-Labeling of Photosynthetic Intermediates.

The kinetics of labeling of the leaf CO₂ plus HCO₃⁻ pool and other intermediates from ¹⁴CO₂ was determined for two species from each of the three C₄ plant subgroups: NADP-malic enzyme-type (*S. vulgare* and *E. crusgalli*), NAD-malic enzyme-type (*E. indica* and *P. milaceum*) and PEP carboxykinase-type (*U. panicoides* and *P. maximum*) (13). All species are grasses (family Gramineae). In all cases the label in the CO₂ plus HCO₃⁻ pool

increased over a period of between 30 and 60 s and then reached a relatively constant value. Figure 1 shows examples of this labeling pattern for one species from each of the C₄ subgroups. The kinetics for labeling of the leaf CO₂ pools were very similar to those found for the C-4 of the C₄ acids malate plus aspartate. They contrasted with the kinetics of labeling seen for labeling of 3-PGA, the phosphorylated sugars pool, and the end products sucrose and starch which showed substantial lag phases and were generally not saturated with ¹⁴C by 120 s. Qualitatively similar kinetic data were obtained for the other three C₄ species examined in the present study. The photosynthesis rate for the six species, determined from ¹⁴CO₂ assimilation, ranged between 3.8 and 7.0 μmol min⁻¹ mg⁻¹ Chl with an average of about 6 μmol min⁻¹ mg⁻¹ Chl.

Included for comparison are the data for the labeling of the CO₂ plus HCO₃⁻ pool in the C₃ grass *Phalaris tuberosa* during steady state photosynthesis (Fig. 2). As expected, labeling of the end products sucrose and starch was preceded by rapid labeling of 3-PGA and phosphorylated sugars. Labeling of the total inorganic carbon pool appeared to be biphasic; about half the total label present at 120 s appeared in less than 15 s. There followed a slower phase of labeling which may not have plateaued even by 120 s. However, as we show later (Table I), the CO₂ pool

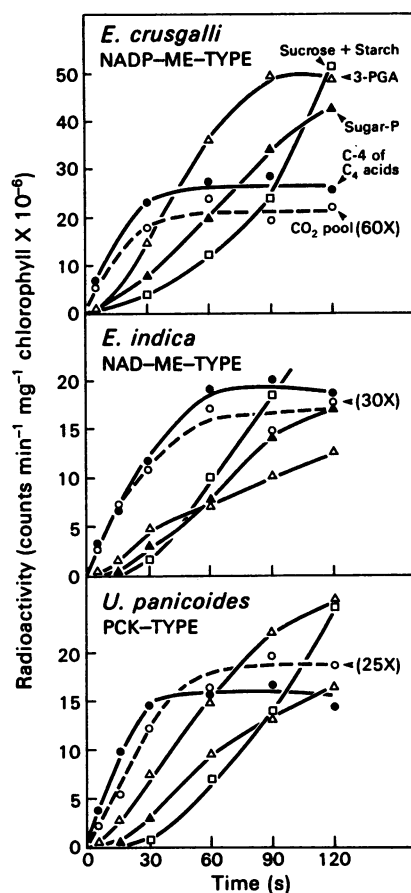


FIG. 1. Time-course of ¹⁴CO₂ assimilation into the leaf CO₂ pool and other intermediates during steady state photosynthesis. The light intensity was 900 μE m⁻² s⁻¹ and the CO₂ concentration about 400 μl L⁻¹. Radioactivity is expressed as liquid scintillation counts (about 80% efficiency). It should be noted that counts in the CO₂ pool have been multiplied by the factor indicated on the figures. Sugar-P represents the combined ¹⁴C of mono- and bisphosphates of hexose and pentose sugars. Other details are provided in the "Materials and Methods" section. In all cases the symbols denote the compounds indicated in the top figure.

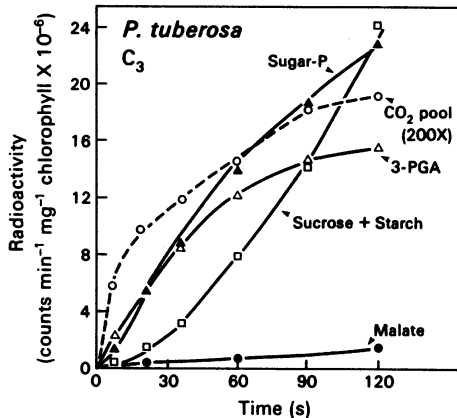


FIG. 2. Time-course of $^{14}\text{CO}_2$ assimilation into photosynthetic intermediates and the internal CO_2 plus HCO_3^- pool in the C_3 plant *P. tuberosa*. It should be noted that the counts in the CO_2 pool have been multiplied by 200. Other conditions were as described in Figure 1 or in "Materials and Methods".

detected in *P. tuberosa* is small compared with the pools determined in the C_4 plants.

CO_2 Pools: Definition and Controls. The total CO_2 plus HCO_3^- present in leaves in the dark or light will include pools in various leaf compartments derived by diffusion equilibration with CO_2 in air. An estimate of the size of this diffusion pool can be made as follows. Assuming that leaves contain 2 mg Chl g^{-1} fresh weight, and the total cytosol, of average pH 7.2, occupies about 20% of the leaf volume (based on our estimates of the average area occupied by cytosol in electron micrographs of five C_4 leaves) it can be calculated that the total CO_2 plus HCO_3^- content at diffusion equilibrium with $350 \mu\text{L L}^{-1} \text{CO}_2$ in air (and thermodynamic equilibrium between CO_2 and HCO_3^- at pH 7.2) will be about $13 \text{ nmol mg}^{-1} \text{Chl}$. Such a value would be expected in darkened leaves where no CO_2 is being assimilated. The substomatal concentration of CO_2 will be lower than external levels in leaves assimilating CO_2 in the light (for example, about 30% of air levels in several C_4 species at high rates of photosynthesis; see Wong *et al.* [28]) and the mesophyll cell concentration of CO_2 would be further reduced. It follows that the steady state pool of CO_2 plus HCO_3^- due to diffusion of CO_2 from air in the light will be reduced to about $4 \text{ nmol mg}^{-1} \text{Chl}$ or less.

One of the controls we routinely employed in the present study (and in the earlier one [10]) was to measure the steady state pool of CO_2 plus HCO_3^- present in darkened leaves. In the dark, the leaf CO_2 plus bicarbonate pool equilibrated with the external $^{14}\text{CO}_2$ pool in less than 20 s and the label in it remained constant for at least 2 min (results not shown). An additional control was provided by determining the size of the CO_2 and HCO_3^- pool developed during photosynthesis of the C_3 grass *Phalaris tuberosa*. The values obtained for these controls are presented (Table I) and discussed in the following section.

The possible influence of the pool of CO_2 bound as carbamate to a regulatory site on RuBP carboxylase (1) was also considered. It can be deduced from the data in Ashton (2) and Ku *et al.* (23) that the active site concentration for RuBP carboxylase is about $90 \text{ nmol mg}^{-1} \text{Chl}$ for C_3 plants and that the value for C_4 plants would be about $22 \text{ nmol mg}^{-1} \text{Chl}$. This value falls just outside the lower end of the range of CO_2 pool sizes we observed for C_4 leaves in the light. The possible influence of this pool will be considered further in the "Discussion" section.

Post-killing decarboxylation of labeled oxaloacetate (12) could generate an artifactual $^{14}\text{CO}_2$ pool. Such decarboxylation would have to be substantial to affect our data since the oxaloacetate pool is only 3 to 4% of the total C_4 acid pool (11, 15); that is, a

pool size comparable to the CO_2 pools recorded in the present study. To prevent this problem oxaloacetate was trapped as the stable hydrazone by killing leaves in 2,4 dinitrophenylhydrazine (also used in earlier studies [11, 15]). The efficiency of this procedure was checked by determining the percentage of added [^{14}C] oxaloacetate, prepared as described by Hatch and Heldt (12), that was decarboxylated during a simulated killing and extraction procedure. Less than 1% of radioactivity was recovered in the CO_2 fraction.

For the purposes of the present paper we will use the following terms to describe the various pools of CO_2 plus HCO_3^- that might exist in leaves. The pool developed by diffusion equilibration with atmospheric CO_2 will be termed the diffusion CO_2 pool. The total CO_2 plus HCO_3^- pool observed in leaves, which will include the diffusion CO_2 pool, will be termed the leaf CO_2 pool. For C_4 plants the leaf CO_2 pool measured in the light and corrected for the diffusion CO_2 pool will be taken to be the pool in bundle sheath cells; it will be termed the bundle sheath CO_2 pool. It should be noted that while the term "CO₂ pool" is used it is accepted that the pool will, in fact, comprise of CO_2 plus HCO_3^- .

Size and Concentration of Leaf CO_2 Pools. Table I provides data on the various CO_2 pools in leaves of the six C_4 species we examined. Calculations assume that when the radioactivity in particular carbons reaches a plateau then the specific activity of these carbons will be equal to that of the external $^{14}\text{CO}_2$. Estimates of the dark diffusion CO_2 pool ranged from 7 to $21 \text{ nmol mg}^{-1} \text{Chl}$ in the different species. This compares with a theoretical value of about $13 \text{ nmol mg}^{-1} \text{Chl}$ calculated above. The diffusion CO_2 pools in the light (calculated as described above from the dark CO_2 diffusion pool) ranged from 2 to $6 \text{ nmol mg}^{-1} \text{Chl}$.

The total leaf CO_2 pools ranged from 18 to $103 \text{ nmol mg}^{-1} \text{Chl}$ and, after subtracting the estimated diffusion CO_2 pool in the light, the range was 15 to $97 \text{ nmol mg}^{-1} \text{Chl}$ (Table I). In accordance with the definitions described above these values will be regarded as a measure of the bundle sheath CO_2 pool. Notably, the total C_4 acid pool involved in photosynthesis (malate plus aspartate measured from the saturating level of ^{14}C in the C_4 carboxyl) was between 20 and 50 times larger than the leaf CO_2 pool (Table I). Assuming a photosynthesis rate of $6 \mu\text{mol CO}_2 \text{ min}^{-1} \text{mg}^{-1} \text{Chl}$ the turnover times for these C_4 acids pools would range between 8 and 25 s.

As a control we also determined the leaf CO_2 pool in the C_3 grass *Phalaris tuberosa* in the light (Table I). As shown in Figure 2 this pool may consist of two distinct components, one saturating in less than 15 s and a second not saturated by 120 s. The rapidly equilibrating component comprised about half the total pool (about $3.8 \text{ nmol mg}^{-1} \text{Chl}$) and was probably the diffusion CO_2 pool in the light. Possible origins of the slower saturating pool will be discussed later. Notably, the size of the rapidly saturating component of the CO_2 pool in the light in the C_3 plant was similar to the theoretical value calculated for photosynthesizing leaves (see above) and within the range of values estimated for the diffusion CO_2 pool for the leaves of C_4 species in the light (average $3.7 \text{ nmol mg}^{-1} \text{Chl}$; Table I). The leaf CO_2 pool in C_4 plants measured in the light averaged more than 15 times this value.

From the values for the CO_2 pool size and estimates of the volumes of bundle sheath cells, cytosol and chloroplasts on a Chl basis (see "Materials and Methods" and footnote to Table I), we could arrive at approximations of the likely concentration of CO_2 plus HCO_3^- in the various bundle sheath cell compartments. The concentrations ranged from 0.15 to 0.97 mM for the whole cell and 0.3 to 1.9 mM if this pool is assumed to be confined to the cytosol. For NADP-malic enzyme-type species values are also given for the chloroplast volume since CO_2 is initially released in the chloroplast in that particular group.

Table I. Inorganic Carbon (CO₂ + HCO₃⁻) Pools in Leaves of C₄ PlantsFor determining pool size it was assumed that at labeling saturation carbons will have the specific activity of the supplied ¹⁴CO₂.

Species	CO ₂ + HCO ₃ ⁻ Pool				Estimated Concentration in Bundle Sheath Cells			C ₄ Acid Pool <i>nmol·mg⁻¹ Chl^e</i>
	Diffusion pool ^a		Pool in light ^b		Whole cell	Cytosol	Chloroplast	
	Observed in dark	Estimated in light	Observed	Corrected value				
			<i>nmol·mg⁻¹ Chl</i>			<i>mM^c</i>		
NADP-ME-type								
<i>E. crusgalli</i>	19	5.7	41	35	0.37	0.74	1.45	1800
<i>S. vulgare</i>	9	2.7	18	15	0.16	0.34	0.63	810
NAD-ME-type								
<i>E. indica</i>	7	2.1	75	73	0.77	1.45		2300
<i>P. miliaceum</i>	10	3.0	39	36	0.35	0.69		1100
PCK-Type								
<i>U. panicoides</i>	21	6.3	103	97	0.99	2.0		2500
<i>P. maximum</i>	8.5	2.5	82	79	0.83	1.65		1100
C ₃ SPECIES								
<i>P. tuberosa</i>			7.1 (3.8) ^d					

^a Steady state CO₂ + HCO₃⁻ pool in equilibrium with CO₂ in air (determined as described in "Materials and Methods"). The pool in the light was estimated from the 'dark' value assuming that substomatal CO₂ in photosynthesizing C₄ leaves is about 30% of the external CO₂ concentration (28) and that liquid phase CO₂ + HCO₃⁻ in the light will be reduced by at least this much. ^b Determined from the CO₂ pool developed in leaves during steady state photosynthesis (Fig. 1; "Materials and Methods") and corrected by subtracting the estimated diffusion CO₂ pool present in the light. ^c Calculated from pool sizes assuming that bundle sheath cell volume is 19% of leaf volume, cytosol is 50% of cell volume, chloroplast stromal volume is 25 μl mg⁻¹ Chl and that 1 g fresh weight of leaf tissues contain 2 mg Chl (see "Materials and Methods" for further details). ^d The CO₂ + HCO₃⁻ pool in the C₃ plant *P. tuberosa* is measured by ¹⁴C incorporation after 120 s photosynthesis in ¹⁴CO₂ (Fig. 2). Kinetics of labeling of this pool showed a rapidly labeled component (shown in brackets, possibly the pool of CO₂ + HCO₃⁻ in diffusion equilibrium with CO₂ in air) and a more slowly saturating pool (considered further in the "Discussion" section). ^e Size of the pool of malate plus aspartate determined from the ¹⁴C in the C-4 carboxyl when this carbon was saturated with label.

Effect of Varying Light on the CO₂ Pool. The CO₂ pool was measured during photosynthesis of *U. panicoides* in light varying between 900 μE m⁻² s⁻¹ (nearly half of full sunlight) and 95 μE m⁻² s⁻¹. In this range there was a near linear response for photosynthesis and a similar response for the leaf CO₂ pool (Fig. 3). The leaf CO₂ pool of 22 nmol mg⁻¹ Chl at 95 μE m⁻² s⁻¹ was equivalent to a bundle sheath cell concentration of about 0.2 mM (based on the assumptions outlined in Table I) and still about 4 times the estimated value for the CO₂ diffusion pool in the light (Table I).

Effect of Varying External CO₂ on the Leaf CO₂ Pool. Radioactivity incorporated into the leaf CO₂ pool was measured following the equilibration of *U. panicoides* leaves in air containing various concentrations of CO₂. With an initial CO₂ concentration similar to that in air (400 μl L⁻¹ CO₂) labeling of the leaf CO₂ pool plateaued at about 60 s (Fig. 4A). This pattern was similar to that shown for leaves of *U. panicoides* and other species in Figure 1. However, interpretation of the results obtained when lower external CO₂ concentrations were used was complicated by substantial proportions of the chamber CO₂ being used during the period that labeling of the leaf CO₂ pool was followed (Fig. 4, B and C). Significantly, in these treatments the ¹⁴C in the leaf CO₂ pool peaked and then declined rather than showing a plateauing of label. Since the specific activity of the CO₂ in the chamber should not decline as the concentration is reduced by assimilation, we take this to mean that the leaf CO₂ pool must decline in size as the external CO₂ concentration declines. In fact, if we assume this to be so, and adjust the observed radioactivity in the leaf CO₂ pool accordingly then the values obtained approach a plateau. We took this plateau value as a measure of the leaf pool size corresponding to the initial external CO₂ concentration. These values were plotted together with the initial photosynthetic rate, against the varying initial concentration of external CO₂ (Fig. 5). There was an almost linear relationship

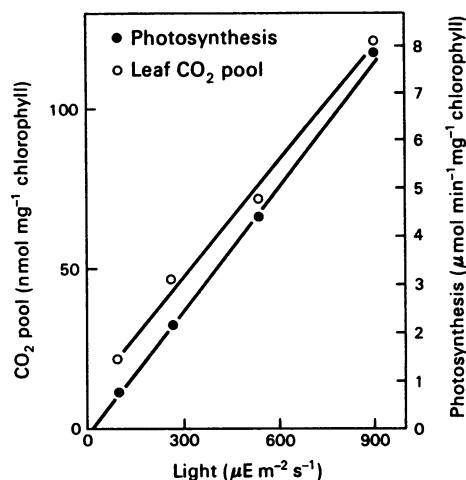


FIG. 3. Effect of varying irradiance on the photosynthesis rate and leaf CO₂ pool of *U. panicoides* leaves. The CO₂ concentration was 400 μl L⁻¹. For other details see "Materials and Methods."

for both the leaf CO₂ pool and the photosynthesis rate as a function of varying external CO₂. At the lowest external CO₂ concentration of 98 μl L⁻¹ the leaf pool of about 14 nmol mg⁻¹ Chl was equivalent to a bundle sheath cell concentration of approximately 0.14 mM based on the assumptions used in Table I.

DISCUSSION

In leaves of C₄ plants the kinetics of labeling of the leaf CO₂ pool from external ¹⁴CO₂ was consistent with the major component being derived from the C-4 carboxyl group of C₄ acids.

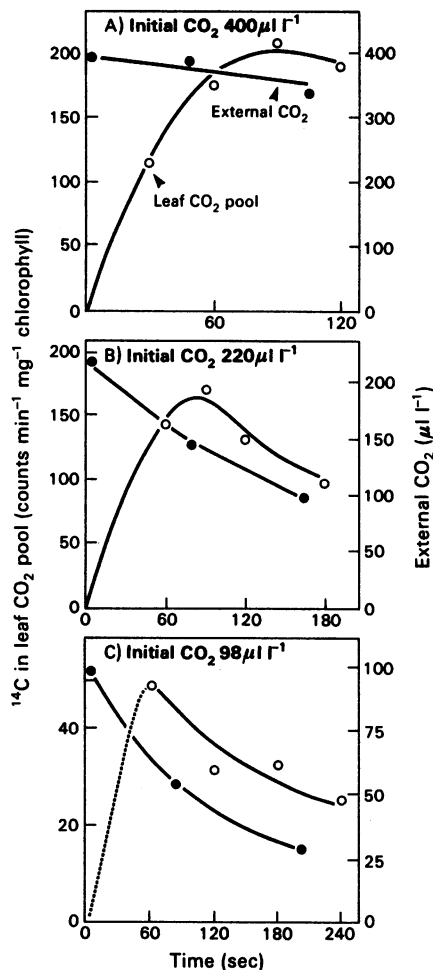


FIG. 4. Time-course for the incorporation of radioactivity into the leaf CO_2 pool of *U. panicoides* leaves and the change in chamber CO_2 levels during photosynthesis. Chamber CO_2 levels were determined by measuring the ^{14}C content of samples of the gas phase removed with a syringe (see "Materials and Methods").

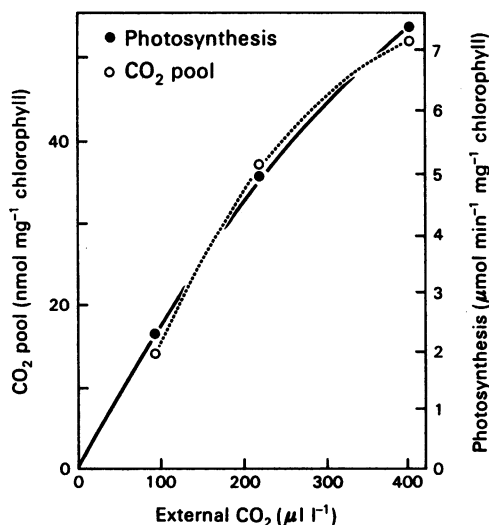


FIG. 5. Effect of varying external CO_2 concentration on the photosynthesis rate and leaf CO_2 pool of *U. panicoides* leaves. Irradiance was $900 \mu\text{E m}^{-2} \text{s}^{-1}$.

These kinetics are very similar to those recorded earlier for the leaf CO_2 pool of the C_4 species *Zea mays* and *Amaranthus edulis* (10). The observed close relationship between the labeling of these two pools would be expected if the relatively small CO_2 pool is derived from the much larger C_4 acid pool (about 20 times higher with turnover times ranging between 8 and 25 s). For all species tested, the leaf CO_2 pool and the C-4 of C_4 acids saturated with ^{14}C between 30 and 60 s, presumably reflecting the similar size of the C_4 acid pools and the similar photosynthesis rates of these species.

Our estimates of the bundle sheath CO_2 pool in C_4 plants were derived after correcting for a CO_2 pool we attributed to diffusion equilibration with CO_2 in air. As briefly mentioned in the "Results" section, the values for this diffusion pool in the light, equivalent to 30% of the dark pool, may be even less in the likely event that the mesophyll cell CO_2 pool is substantially less than the substomatal CO_2 levels (Table I; "Results"). However, a counteracting effect might be the increased pH of the chloroplast stroma in the light which would result in higher steady levels of HCO_3^- in that particular component of the leaf liquid phase. Our calculations indicate that this pH shift would not have a major quantitative influence on total leaf CO_2 , and this view is supported by the low level of labeling of the CO_2 pool observed in the leaves of the C_3 plant *P. tuberosa* in the light.

The results obtained with *P. tuberosa* leaves also make it unlikely that the CO_2 bound as carbamate to a regulatory site on RuBP carboxylase was a significant interfering factor in our measurements. The calculations in the "Results" section shows that, even if all the regulatory sites on RuBP carboxylase were carbamylated, this would represent a pool smaller than the CO_2 pool observed in most C_4 plants in the light. In any case, there is evidence from studies with isolated chloroplasts (3) that the turnover of this pool is slow compared with the time scale of our experiments. Furthermore, the higher RuBP levels anticipated to prevail in intact leaves during steady state photosynthesis would be likely to further reduce the turnover of this bound CO_2 (19, 20). It is possible that the component of the CO_2 pool that slowly saturated with ^{14}C in the illuminated leaves of the C_3 plant *P. tuberosa* represented the regulatory CO_2 on RuBP carboxylase.

Estimates of the concentration of the CO_2 plus HCO_3^- pool in bundle sheath cells varied depending on species and the assumptions made about compartmentation of this pool. With higher light and external CO_2 close to that normally in air, the estimates ranged from more than 1 mM to about 0.15 mM (Table I). The leaf CO_2 pool, and hence the concentration, was reduced together with photosynthesis as either light or the external CO_2 concentration was reduced. It is generally accepted that by concentrating CO_2 in bundle sheath cells the C_4 pathway serves to suppress the oxygenase activity of RuBP carboxylase and hence photorespiration (14, 24). The critical factor for this effect is the high ratio of CO_2 to O_2 in bundle sheath cells where RuBP carboxylase is exclusively located. It is therefore important to know the concentration of CO_2 , as such, in bundle sheath cells rather than the total CO_2 plus HCO_3^- . Of course, as indicated earlier, our method for leaf CO_2 pool analysis does not distinguish between these two forms of inorganic carbon. In the following section this problem is considered. A model is developed which supports the view that CO_2 as such would be the major inorganic carbon species in bundle sheath cells during steady state photosynthesis.

RuBP carboxylase uses CO_2 and not HCO_3^- as a substrate for carboxylation (5). There are conflicting reports in the literature about the form of inorganic carbon released by the three C_4 acid decarboxylases involved in C_4 photosynthesis; these reports are discussed in the preceding paper which also presents clear evidence that CO_2 , as such, is the product for all three enzymes (17). The question then arises as to what extent a bicarbonate pool develops in this system. Most green cells contain high levels of carbonic anhydrase and the CO_2 and HCO_3^- components of

the inorganic carbon pool would usually be assumed to be in thermodynamic equilibrium. However, bundle sheath cells of C₄ plants apparently contain little or no carbonic anhydrase (22). Our recent unpublished studies (JN Burnell, MD Hatch) support this conclusion; the low levels of carbonic anhydrase recorded in bundle sheath cell extracts from six C₄ species could be entirely accounted for by trace contamination by mesophyll cells. Thus, equilibration between CO₂ and HCO₃⁻ in bundle sheath cells might proceed only at the noncatalyzed rate, or a rate of this order.

To predict the ratio of CO₂ to HCO₃⁻ in bundle sheath cells we developed a model based on the scheme shown in Figure 6. For this model we assume a steady state situation such that for the CO₂ in bundle sheath cells

$$\frac{d[\text{CO}_2]}{dt} = v_1 - v_2 - v_3 - v_4 = 0$$

where v_1 is the rate of C₄ acid decarboxylation, v_2 is the rate of CO₂ assimilation, and v_3 and v_4 are the diffusion efflux velocities of CO₂ and HCO₃⁻ from the bundle sheath cells. It should be noted that at the steady state v_4 will equal the rate of CO₂ hydration to HCO₃⁻ minus the rate of the reverse reaction. Using the assumptions listed in the legend we arrived at the values for pool sizes and reaction rates indicated on the scheme by an empirical procedure involving repetitive trials. Briefly, the ratio of CO₂ to HCO₃⁻ in the bundle sheath cell inorganic carbon pool is altered until the calculated rate of CO₂ hydration to give

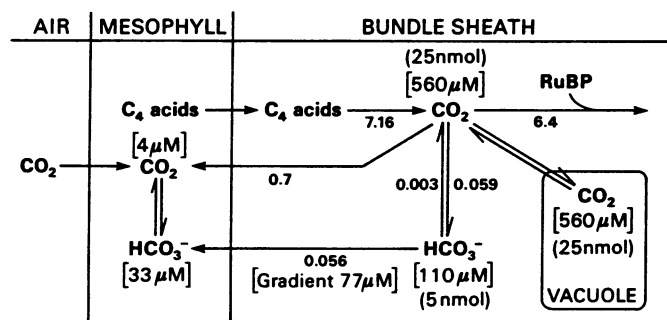


FIG. 6. Model for predicting the ratio of CO₂ to HCO₃⁻ in bundle sheath cells during steady state photosynthesis. Assumptions for the calculation shown are: photosynthesis rate of 6.4 μmol min⁻¹ mg⁻¹ Chl and a bundle sheath CO₂ pool of 55 nmol mg⁻¹ Chl (average for the six species examined in the present study); bundle sheath cells occupy 18% of the leaf volume, the cytosol (includes chloroplasts and mitochondria) occupies 50% of the bundle sheath cell volume (*i.e.* vacuole occupies remaining 50%), and leaves contain 2 mg Chl per g fresh weight (see "Materials and Methods" for further details about these assumptions); the resistance to symplastic diffusion across the mesophyll-bundle sheath interface (via plasmodesmata) is such that with a diffusion coefficient of $0.8 \times 10^{-5} \text{ cm}^2 \text{ s}^{-1}$ a gradient of 1.9 mm will generate a flux of $1 \mu\text{mol min}^{-2} \text{ mg}^{-1} \text{ Chl}$ (14); rate constant for CO₂ → HCO₃⁻ is $3.8 \times 10^{-2} \text{ s}^{-1}$ and for HCO₃⁻ → CO₂ is $1.1 \times 10^{-2} \text{ s}^{-1}$ at pH 7 (7); diffusion coefficient for CO₂ and HCO₃⁻ from Kigoshi and Hashitani (21) and for C₄ acids from Weast (27). For the values shown in the scheme we also assumed that the bundle sheath cells contained no carbonic anhydrase, that the mesophyll CO₂ concentration would be 4 μM (C_i approximately 30% of C_a [28]) giving HCO₃⁻ concentration of about 33 μM at pH 7.2, that CO₂ would efflux by the same plasmodesmatal path as HCO₃⁻ and C₄ acids (14), and that cytosolic CO₂ would equilibrate with the vacuolar space but that there would be no HCO₃⁻ in the vacuole due to the low pH. The velocities shown in bold numbers are expressed as μmol min⁻¹ mg⁻¹ Chl. Pool sizes in nmol mg⁻¹ Chl are shown in curved brackets and concentrations of pools in square brackets.

HCO₃⁻ is equal to the rate of HCO₃⁻ efflux plus the rate of conversion of HCO₃⁻ back to CO₂; that is, the condition giving a steady state with respect to the inorganic carbon pools. With the particular set of assumptions used for Figure 6 the velocities balanced with CO₂ comprising about 90% of the total inorganic carbon pool of the cell (equivalent to cytosolic CO₂ comprising about 83% of the total cytosolic inorganic carbon pool). By contrast, if CO₂ and HCO₃⁻ reached thermodynamic equilibrium at either pH 7.2 or at pH 8.0 the proportion of inorganic carbon as CO₂ in the cytosol would be only about 11 and 2%, respectively (calculated from data in Ref. 26).

One of the most critical features of the C₄ pathway besides the concentration of CO₂ in the bundle sheath cells is the extent to which CO₂ released in bundle sheath cells leaks back to mesophyll cells (14). Among other things, this leak will determine how efficiently the C₄ pathway operates in an energetic sense and, in particular, it will directly affect the quantum yield. With the assumptions outlined in the legend of Figure 6 the calculated leak rates of CO₂ plus HCO₃⁻ from bundle sheath cells represented about 11% of the CO₂ originally released in the bundle sheath cells. Of course this requires that the C₄ acid cycle must turn over about 11% faster than RuBP carboxylase and the subsequent steps of the Photosynthetic Carbon Reduction cycle. This value is similar to the one calculated by Hatch and Osmond (14) for the so-called back-flux of CO₂ plus HCO₃⁻ based on earlier data (10) but less than other models predict (7).

We also assessed the effects of varying the critical assumptions in Figure 6 on the steady state ratios of CO₂ to HCO₃⁻ and the inorganic carbon leak rates (percent of CO₂ released in bundle sheath cells that leaks back to mesophyll cells). The results are summarized in Table II. The CO₂ component of the total inorganic carbon pool was calculated to be as high as 99% (assuming vacuole 90% of cell volume) but, notably, was never lower than 55%. The latter value was obtained when the rate constant for conversion of CO₂ to HCO₃⁻ was assumed to be 10 times the uncatalyzed rate (through catalysis by carbonic anhydrase). Calculated CO₂ leak rates were most affected by the assumption made about the resistance to diffusion between bundle sheath and mesophyll cells. If values for resistance of half or double that assumed for the calculations in Figure 6 were taken then the leak rates for CO₂ either increased to 19% or decreased to 5%, respectively. These analyses clearly support the view that the

Table II. Effects of Varying the Assumptions Made in Figure 6 on Estimates of the Proportion of CO₂ in Inorganic Carbon Pools and the CO₂ Leak Rate from Bundle Sheath Cells

Assumptions	% of Inorganic Carbon as CO ₂		Leakage of CO ₂ % ^a
	Cell	Cytosol	
As in Figure 6	91	83	11
CO ₂ ⇌ HCO ₃ ⁻ rate constants for pH 8 ^b	90	81	11
CO ₂ ⇌ HCO ₃ ⁻ rate constants 10 times higher	55	38	12
Photosynthesis rate 1/10	81	66	17
No vacuole	74	74	10
Vacuole 90% of cell volume	99	93	12
Half-diffusion resistance ^c	93	88	19
Twice diffusion resistance ^c	86	75	6

^a Proportion of CO₂ released in bundle sheath cells that diffuses back to mesophyll as CO₂ or HCO₃⁻. ^b At pH 8.45 $\times 10^{-2} \text{ s}^{-1}$ for CO₂ → HCO₃⁻ and $1.2 \times 10^{-3} \text{ s}^{-1}$ for HCO₃⁻ → CO₂ (see legend of Fig. 6). ^c Refers to diffusion resistance between mesophyll and bundle sheath cells (see legend of Table I).

CO₂ concentration in bundle sheath cells of C₄ plants during steady state photosynthesis is likely to remain much higher than expected if thermodynamic equilibrium with HCO₃⁻ is approached. For the considerations in the following discussion it might be conservatively assumed that the CO₂ component of our measured leaf inorganic carbon pools would be at least half of the total pool.

Taking an atmospheric CO₂ concentration of 350 μL L⁻¹ and the substomatal CO₂ concentration during steady state photosynthesis for C₄ and C₃ species as 30 and 66%, respectively, of the atmospheric concentration (28), the liquid phase CO₂ concentrations in equilibrium with these substomatal concentrations would be about 3 μM for C₄ leaves and 6.6 μM for C₃ leaves at 25°C. During the present study we estimated concentrations of the bundle sheath inorganic carbon pool in the range between 1.5 and 0.15 mM depending on species and factors such as light or CO₂. If such a pool comprised of CO₂ and HCO₃⁻ in thermodynamic equilibrium at pH 8.2 (likely stromal pH in the light [16], and maximum value obtained for C₄ mesophyll chloroplasts in the light [S Boag, MD Hatch, unpublished data]) then the concentration of the CO₂ component would range between 15 and 1.5 μM (*i.e.* about 1% of the total [26]). Such CO₂ concentrations are of the same order as those prevailing in the mesophyll cells of C₃ plants during photosynthesis and should allow substantial O₂ effects on photosynthesis and also readily observed photorespiration. On the other hand, if more than half these inorganic carbon pools are comprised of CO₂, as our calculations suggest, then the CO₂ concentration will range between 750 and 75 μM at a minimum; these concentrations are between 10 and 100 times those prevailing in mesophyll cells of C₃ plants. Such concentrations give ratios of CO₂ to O₂ of at least 10 times those in C₃ plants and should effectively eliminate the oxygen-induced effects on photosynthesis typical of C₃ plants (1). This conclusion is supported by a wide variety of observations indicating negligible photorespiration and related oxygen effects on photosynthesis in C₄ plants (6, 8, 14, 24).

It has been suspected that the high resistance to gas diffusion between mesophyll and bundle sheath cells which allows the concentrating of CO₂ may result in elevated concentrations of O₂ in bundle sheath cells during photosynthesis (7). The exceptionally high leaf CO₂ pools we recorded for some species may, in part, be necessary to counteract these high oxygen concentrations. It is notable in this regard that NADP-malic enzyme type C₄ plants contain little PSII activity in bundle sheath cells and hence would generate little O₂. This may explain why we found the CO₂ pools in the species from this group to be among the lowest in the range of values recorded.

With respect to the factors controlling photosynthesis we assume that where photosynthesis is limited by CO₂ PEP carboxylase activity is a major limiting step. However, it should be noted that as external CO₂ is reduced the leaf CO₂ pool declines together with photosynthesis such that at 98 μL L⁻¹ external CO₂ the total inorganic carbon pool in *U. panicoides* was only about 140 μM (Fig. 5). The CO₂ component of this pool may only be about half of the total (or possibly less at low rates of photosynthesis; see above and Table II). This brings the CO₂ concentration in the same range as the published K_m CO₂ values for RuBP carboxylase from C₄ species (29) and apparent K_m value would be increased further in the presence of high concentrations of oxygen. Thus, it is possible that RuBP carboxylase contributes to the limitation of photosynthesis in these leaves. Alternatively, turnover through this enzyme may simply be coordinated with the prevailing PEP carboxylase activity by the changing CO₂ pool size in bundle sheath cells.

LITERATURE CITED

- ANDREWS JA, G LORIMER 1987 Rubisco, structure, mechanism and prospects for improvement. In MD Hatch, CB Osmond, eds, The Biochemistry of Plants. A Comprehensive Treatise, Vol 10, Photosynthesis. Academic Press, New York, pp 131-218
- ASHTON AR 1982 A role for ribulose bisphosphate carboxylase as a metabolite buffer FEBS Lett 145: 1-7
- BELKNAP WR, AR PORTIS 1986 Exchange properties of the activator CO₂ of spinach ribulose 1,5-bisphosphate carboxylase. Plant Physiol 80: 707-710
- BJORKMAN O 1971 Comparative photosynthetic CO₂ exchange in higher plants. In MD Hatch, CB Osmond, RO Slatyer, eds, Photosynthesis and Photorespiration. Wiley-Interscience, New York, pp 18-23
- COOPER TG, D FILMER, M WISNICK, MD LANE 1969 Active species of 'CO₂' utilized by ribulose diphosphate carboxylase. J Biol Chem 244: 1081-1083
- EDWARDS GE, DA WALKER 1983 C₃, C₄: Mechanisms and Cellular and Environmental Regulation of Photosynthesis. Blackwell Scientific Publication, London
- FARQUHAR GD 1983 On the nature of carbon isotope discrimination in C₄ species. Aust J Plant Physiol 10: 205-226
- FURBANK RT, MR BADGER 1982 Photosynthetic oxygen exchange in attached leaves of C₄ monocotyledons. Aust J Plant Physiol 9: 553-558
- HATCH MD 1971 Mechanism and function of the C₄ pathway of photosynthesis. In MD Hatch, CB Osmond, RO Slatyer, eds, Photosynthesis and Photorespiration. Wiley-Interscience, New York, pp 139-152
- HATCH MD 1971 The C₄-pathway of photosynthesis: evidence for an intermediate pool of carbon dioxide and the identity of the donor C₄ acid. Biochem J 125: 425-432
- HATCH MD 1979 Mechanism of C₄ photosynthesis in *Chloris gayana*. Pool sizes and the kinetics of ¹⁴CO₂ incorporation into 4-carbon and 3-carbon intermediates. Arch Biochem Biophys 194: 117-127
- HATCH MD, HW HELDT 1985 Synthesis storage and stability of [¹⁴C] oxaloacetic acid. Anal Biochem 145: 393-397
- HATCH MD, T KAGAWA, S CRAIG 1975 Subdivision of C₄ pathway species based on differing C₄ acid decarboxylating systems and ultrastructural features. Aust J Plant Physiol 2: 111-128
- HATCH MD, CB OSMOND 1976 Compartmentation and transport in C₄ photosynthesis. In CR Stocking, U Heber, eds, Encyclopedia of Plant Physiology, New Series Vol 3, Transport in Plants. Springer-Verlag, Berlin, pp 144-184
- HATCH MD, CR SLACK 1966 Photosynthesis in sugarcane leaves. A new carboxylation reaction and the pathway of sugar formation. Biochem J 101: 103-111
- HELDT HW, K WERDEN, M MILOVANCEV, G GELLER 1973 Alkalinization of the chloroplast stroma caused by light-dependent proton flux into the thylakoid space. Biochem Biophys Acta 314: 224-241
- JENKINS CLD, JN BURNELL, MD HATCH 1987 Form of inorganic carbon involved as a product and as an inhibitor of the C₄ acid decarboxylases operating in C₄ photosynthesis. Plant Physiol 85: 952-957
- JOHNSON HS, MD HATCH 1969 The C₄ dicarboxylic acid pathway of photosynthesis. Identification of intermediates and products and evidence for the route of carbon flow. Biochem J 114: 127-134
- JORDON DB, R CHOLLET 1983 Inhibition of ribulose bisphosphate carboxylase by substrate ribulose bisphosphate. J Biol Chem 258: 13742-13758
- JORDON DB, R CHOLLET, WL OGREN 1983 Binding of phosphorylated effectors by active and inactive forms of ribulose 1,5-bisphosphate carboxylase. Biochemistry 22: 3410-3418
- Kigoshi K, T Hashitani 1963 The self-diffusion coefficients of carbon dioxide, hydrogen carbonate ions and carbonate ions in aqueous solutions. Bull Chem Soc Jpn 36: 1372
- KU MSB, GE EDWARDS 1975 Photosynthesis in mesophyll protoplasts and bundle sheath cells of various types of C₄ plants. Z Pflanzenphysiol 77: 16-32
- KU MSB, MR SCHMITT, GE EDWARDS 1979 Quantitative determination of RuBP carboxylase protein in leaves of several C₃ and C₄ plants. J Exp Bot 30: 89-98
- LORIMER GH, JA ANDREWS 1981 The C₂ chemo- and photorespiratory carbon oxidation cycle. In MD Hatch, NK Boardman, eds, The Biochemistry of Plants, Vol 8, Photosynthesis. Academic Press, New York, pp 329-374
- SCHÜRMAN P 1969 Separation of phosphate esters in algal extracts by thin-layer electrophoresis and chromatography. J Chromatogr 39: 507-509
- UMBREIT WW, RH BURRIS, JF STAUFFER 1964 Manometric Techniques, Ed 4. Burgess Publishing Co., Minneapolis
- WEAST RC (ed) 1963 Handbook and Chemistry and Physics, Ed 49. Chemical Rubber Co., Cleveland
- WONG SC, IR COWAN, GD FARQUHAR 1985 Leaf conductance in relation to rate of CO₂ assimilation. I. Influence of nitrogen nutrition, phosphorus nutrition, photon flux density, and ambient partial pressure of CO₂ during ontogeny. Plant Physiol 78: 821-825
- YEOH H, P HATTERSLEY 1985 K_m (CO₂) values for ribulose 1,5-bisphosphate carboxylase in grasses of different C₄ types. Phytochemistry 24: 2277-2279